Theoretical Spectroscopic Characterization at Low Temperatures of Dimethyl Sulfoxide: The Role of Anharmonicity

ARTICLE *in* THE JOURNAL OF PHYSICAL CHEMISTRY A · AUGUST 2015

Impact Factor: 2.69 · DOI: 10.1021/acs.jpca.5b06941 · Source: PubMed

THE JOURNAL OF PHYSICAL CHEMISTRY A

Article

pubs.acs.org/JPCA

Theoretical Spectroscopic Characterization at Low Temperatures of Dimethyl Sulfoxide: The Role of Anharmonicity

Published as part of The Journal of Physical Chemistry A virtual special issue "Spectroscopy and Dynamics of Medium-Sized Molecules and Clusters: Theory, Experiment, and Applications".

M. L. Senent* and S. Dalbouha†

Departamento de Química y Física Teóricas, Instituto de Estructura de la Materia, IEM-C.S.I.C., Serrano 121, Madrid 28006, Spain

A. Cuisset‡ and D. Sadovskii§

Laboratoire de Physico-Chimie de l'Atmosphère, Maison de la Recherche en Environnement Industriel, Université du Littoral − Côte d'Opale, 59140 Dunkerque, France

ABSTRACT: The structural and spectroscopic parameters of dimethyl sulfoxide (DMSO) are predicted from CCSD(T)-F12 calculations that can help to resolve the outstanding problem of the rovibrational spectroscopy. DMSO is a near oblate top that presents a trigonal pyramidal geometry. Rotational parameters are determined at the equilibrium and in selected vibrational states. For the ground state, the rotational constants were calculated to be A_0 = 7031.7237 MHz, B_0 = 6920.1221 MHz, and C_0 = 4223.3389 MHz, at few megahertz from the previous experimental measurements. Ab initio calculations allow us to assert that DMSO rotational constants are strongly dependent on anharmonic effects. Asymmetry increases with the vibrational energy. Harmonic frequencies, torsional parameters, and a two-dimensional potential energy surface (2D-PES) focused to describe the internal rotation of the two methyl groups are determined at the CCSD(T)-F12 level of theory. For the medium and small amplitude motions, anharmonic effects are estimated with MP2 theory getting an excellent agreement with experimental data for the ν_{11} and ν_{23} fundamentals. Torsional energies and transitions are computed variationally form the 2D-PES that denotes strong interactions between both internal tops. The vibrationally corrected V_3 torsional barrier is evaluated to be 965.32 cm^{-1}. The torsional splitting of the ground vibrational state has been estimated to be lower than 0.01 cm^{-1}. Although the ν_{13} torsional fundamental is found at 229.837 cm^{-1} in good agreement with previous assessment, there is not accord for the low intense transition ν_{24}. A new assignment predicting ν_{24} to lie between 190 and 195 cm^{-1} is proposed.

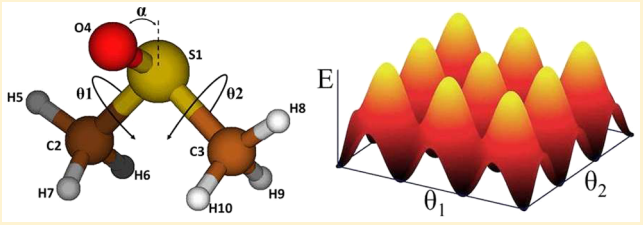

INTRODUCTION

Dimethyl sulfoxide (DMSO, $(CH_3)_2SO$) is an organosulfur compound with varied practical applications. Frequently, it is used as a solvent for chemical reactions involving salts. In medicine, it is predominantly used as a topical analgesic, as anti-inflammatory, and as antioxidant. In the gas phase, DMSO can play important roles in the sulfur atmospheric chemistry because it is an important product of dimethyl sulfide (CH_3SCH_3, DMS) photooxidation in the oceanic atmosphere.[1,2]

The singular structure and dynamic properties of DMSO lead to intricate assignments of the rotational and high-resolution vibrational spectra[3−8] for which the definition of an efficient effective Hamiltonian is not straightforward. On the one hand, the most stable geometry is a C_s trigonal pyramidal structure where two interacting methyl groups confer nonrigid properties. If internal rotation is considered, the molecule can be classified in the G_{18} Molecular Symmetry Group (MSG).[9] On the other hand, DMSO is a near oblate top which equilibrium rotational constants obey the $A_e \sim B_e > C_e$ relation. These rotational parameters are strongly dependent on the anharmonic and centrifugal distortion effects. Cuisset et al.[3−6] have emphasized the phenomenon of gyroscopic destabilization after observing the low-frequency bending mode high-resolution spectra recorded with the synchrotron SOLEIL. Characteristic doublets for symmetric tops are observed for low values of the J angular momentum, whereas patterns of four-degenerate states appear when the centrifugal distortion effect increases (for J > 40). Furthermore, Cuisset et al.[4] provided rotational parameters of the ground vibrational state and five low-energy excited states. They used the S-IIIr reduction for the analysis. Margulès et al.,[7] who measured the millimeter and the submillimeter wave spectra of the ground vibrational state up to

Received: July 17, 2015
Revised: August 26, 2015
Published: August 27, 2015

DOI: 10.1021/acs.jpca.5b06941
J. Phys. Chem. A 2015, 119, 9644−9652

660 GHz, concluded that a good fit requires a good choice of the Watson reduced representation.[10]

During the 1960s, measurements of the low-resolution vibrational spectra in gas and liquid phases (IR and Raman) were motivated by the increasing interest in DMSO complexes and the applications as solvent. Horrocks and Cotton[11] recorded both spectra in the 250−4000 cm^{-1} region. Salonen et al.[12] performed measurements in the skeletal modes observing bands below 200 cm^{-1} (at 115, 150, and 188 cm^{-1}), and later, Forel and Tranquille[13] observed the 250 and 4000 cm^{-1} region and the low-frequency region between 400 and 200 cm^{-1}. These authors employed their own previous experimental data[14] to fit an empirical force field. They did not detect and did not predict the low-frequency patterns obtained by Salonen.[12]

One year later, in 1972, Geiseler and Hanschmann[15] observed the vibrational spectra in gas and liquid phases above 600 cm^{-1}. More recent findings are those of Typke[16] and Typke and Dakkouri[17] who derived a new semiempirical force field using previous experimental data and scaled ab initio calculations. The rotational constants of various isotopomers were employed by Typke[16] to obtain structural parameters at the vibrational ground state.

The first gas phase high-resolution far-infrared spectrum was undertaken recently with the AILES beamline of SOLEIL,[3−5,18] observing the rovibrational bands ν_{11} (SO in-plane bending) and ν_{23} (OSC out-of-plane bending). Band centers were identified at 376.751 and 323.988 cm^{-1}, respectively. Additionally, Cuisset et al.[4] calculated the CSC bending mode (ν_{12}) and the two methyl torsion (ν_{13} and ν_{24}) fundamentals to be 308, 231, and 207 cm^{-1}, using B3LYP/6-311+G(3df,2p) theory.

However, the assignment of two torsional fundamentals of DMSO is uncertain. Both fundamental vibrations are weakly infrared active although ν_{13} is expected to be more intense than ν_{24}. The location of the band centers (231 and 207 cm^{-1}) was first established by Dreizler and Dendl[19] in 1965, after the analysis of the rotational spectrum. From fitted semiempirical force fields, both fundamentals were predicted to lie at the same frequency (212 cm^{-1})[15] and at 219.5 and 201.9 cm^{-1}.[17] To our knowledge, there are no available results derived from very accurate ab initio calculations or high-resolution measurements in the 100−250 cm^{-1} region.

The present paper seeks to obtain a new spectroscopic characterization of DMSO using highly correlated ab initio calculations. To obtain reliable properties, we used the very accurate explicitly correlated coupled cluster method CCSD-(T)-F12b[20,21] for the determination of structures and potential energy surfaces because, as has been pointed out,[22] this method provides excellent rotational and torsional parameters. Along the paper, we combine vibrational second-order perturbation theory (VPT2) and a variational procedure of reduced dimensionality.[23−26] VPT2 was employed to obtain parameters of the symmetric (S, I^r) and asymmetric (A, I^r) reduced Hamiltonians. The variational procedure was applied to the torsional analysis and to explore the far-infrared region.

COMPUTATION DETAILS

The electronic structure calculations were performed with the MOLPRO[27] and GAUSSIAN[28] packages. The equilibrium structure as well as the harmonic fundamentals and the two-dimensional potential energy surface were determined using the explicitly correlated couple cluster theory, CCSD(T)-F12b, implemented in MOLPRO,[20,21] whereas the anharmonic corrections of the vibrational frequencies and rotational parameters were achieved using the second-order perturbation theory (VPT2) implemented in Gaussian.[29] The anharmonic force field was determined using second-order Möller−Plesset theory and Dunning's aug-cc-pVTZ basis set[30] (denoted in this paper by AVTZ).

For the explicitly correlated calculations, the MOLPRO default options were selected. The atomic orbitals were described by the cc-pVTZ-F12 basis set of Peterson et al.[31] (denoted in this paper by VTZ-F12) in connection with the corresponding basis sets[32] for the density fitting and the resolutions of the identity.

To obtain reliable equilibrium rotational constants, the core−valence electron correlation effects were introduced using CCSD(T) (coupled-cluster theory with singles and doubles substitutions, augmented by a perturbative treatment of triple excitations)[33] and the cc-pCVTZ basis set.[34,35]

Finally, to explore the torsional structure and to simulate the far-infrared spectra, we used a variational procedure for a space of reduced dimensionality as is implemented in the original Fortran code ENEDIM.[36] This code allows us to determine the kinetic parameters of a Hamiltonian of reduced dimensionality starting from the geometries optimized at the CCSD(T)-F12b level of theory. The corresponding potential energy surface (PES-2D) is determined in a linear fit of the corresponding CCSD(T)-F12b total electronic energies. The Hamiltonian is solved variationally using ENEDIM to obtain torsional energy levels and frequencies.

SYMMETRY OF DMSO

As we said in the Introduction, the most stable geometry is a trigonal pyramidal structure that can be classified in the C_s group. If internal rotation is considered, the molecule can be classified in the G_{18} Molecular Symmetry Group (MSG).[9] The MSG G_{18} is also the group of the dimethylamine previously studied by some of us in a series of papers whose aim was to determine torsional structures and the interactions between torsional modes and medium amplitude vibrations.[9,37−39] G_{18} contains six symmetry species. The nondegenerate A_1 and A_2 are symmetric and antisymmetric representations with respect to the reflection in the C_s plane. The pseudodegenerate representations E_1 and E_2 include a complex conjugate pair of one-degenerate representations E_{1a} and E_{1b}, E_{2a} and E_{2b}. E_3 is a two-degenerate representation and G contains a complex conjugate pair of two-degenerate representations G_{1a}, G_{1b}, G_{2a}, and G_{2b}.

The SO in-plane bending mode does not contribute to the nonrigidity because the inversion barrier is relatively high (51.7 kcal/mol, MP2/6-31G(d,p)). Thus, each vibrational energy level is considered to split into two groups of nine components each, which are the number of wells in the potential energy surface.

RESULTS AND DISCUSSION

Molecular Structure of DMSO and the Rotational Constants. Figure 1 represents the most stable geometry of DMSO. Because all the nine minima of the potential energy surface are equivalent, the geometry corresponds to the unique conformer of the molecule. The figure gives the atom labeling and the large amplitude coordinates.

Table 1 displays the equilibrium structural parameters and the equilibrium rotational constants calculated using CCSD-

DOI: 10.1021/acs.jpca.5b06941
J. Phys. Chem. A 2015, 119, 9644−9652

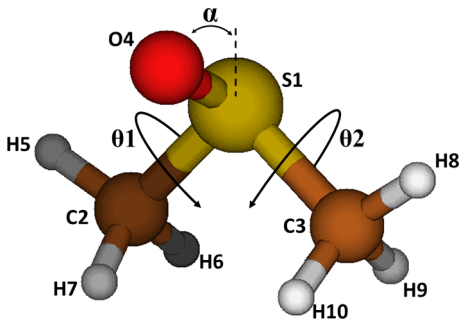

Figure 1. Equilibrium geometry of DMSO.

(T)-F12 in connection with the VTZ-F12 basis set. The three components of the dipole moment with respect to the principal axis determined with MP2/AVTZ are also shown. Although all these data correspond to the minimum energy geometry, ab initio internal coordinates are compared with those of Typke[16] determined using the experimental rotational constants of eight isotopomers measured at the ground vibrational states. In fact, due to the high accuracy of equilibrium rotational constants estimated in the present manuscript, the reported equilibrium parameters are most likely more accurate than the ones from ref 16.

The C−S and O−S bond distances were found to be 1.8015 and 1.4797 Å and can be compared with the values of Typke[16] of 1.799 and 1.485 Å. The α coordinate (angle between the O−S bond and the CSC angle) is in very good agreement (64.9° (this work) and 64.49°[16]).

Table 1 displays the CCSD(T)-F12b equilibrium rotational constants (B_e) and the vibrationally corrected parameters (B_0) obtained combining CCSD(T)-F12b, CCSD(T), and MP2 theories. All the steps followed to determine B_0 from B_e are summarized in Tables 1 and 2. For this purpose, we considered the equation

$$B_0 = B_e + \Delta B_e^{core} + \Delta B^{vib} \quad (1)$$

Here, ΔB^{vib} represents the vibrational contribution to the rotational constants derived from the VPT2 α_r^i vibration−rotation interaction parameters determined using the MP2/AVTZ cubic force field (see below). ΔB_e^{core} regards the core−valence−electron correlation effect on the equilibrium parameters. It was computed at the CCSD(T)/cc-pCVTZ level of theory as the difference between B_e(CV) (calculated correlating both core and valence electrons) and B_e(V) (calculated correlating just the valence electrons). For B_e(CV), two possible cases depending on N (N = number of inner-orbitals excluded from the correlation calculation), were considered: (1) all the core electrons were correlated (N = 0) and (2) the 1s electron of the sulfur atom was not correlated (N = 1). Both cases lead to similar results. Details of all these steps are summarized in Table 2.

The rotational constants of Table 1 calculated by doing N^a = 0 (A_0 = 7031.7237 MHz, B_0 = 6920.1221 MHz, and C_0 = 4223.3389 MHz) were computed in a very good agreement with the experimental results of Cuisset et al.[4] (A_0 = 7036.5822165(234) MHz, B_0 = 6910.8301279(228) MHz, and C_0 = 4218.776511(44) MHz). An excellent agreement is observed for the average (A_0 + B_0)/2 (6974.8879 MHz (this work); 6973.7062 MHz[4]).

It can be confirmed that at the equilibrium geometry, DMSO behaves as a near symmetric top losing symmetry with the vibrational distortion. For example, at equilibrium, Ray's asymmetry parameter κ = 0.965484 whereas, at the ground vibrational state, κ = 0.920523 (κ represents the Ray's asymmetry parameter defined as $\kappa = (2A - B - C)/(A - C)$). As was expected, there is excellent agreement (~2 MHz) between our calculations and the experimental data[4] for the (A_0 + B_0)/2 parameter and there is very good agreement for the rotational constants (5, 9, and 4 MHz). Whereas the average depends basically on the very accurate CCSD(T)-F12b structure, the A_0−B_0 gap depends on the less accurate MP2 α_r^i vibration−rotation interaction parameters. Unfortunately, the size of the molecules impedes the determination of the cubic force fields using highly correlated methods.

Full Dimensional Vibrational Analysis: Raman and Infrared Spectra. An anharmonic force field, containing quadratic, cubic, and quartic terms, has been computed at the

Table 1. Total Electronic Energy, Dipole Moment, Rotational Constants, and Structural Parameters (Distances in Å and Angles in Degrees) of the Equilibrium Geometry of DMSO

parameters	CCSD(T)-F12 VTZ-F12	exp[4]	parameters	CCSD(T)-F12 VTZ-F12	ref 16[a]
E (au)	−552.579381		C2S1═C3S1	1.8015	1.799
θ_1 (deg)	0.0		O4S1	1.4797	1.485
θ_2 (deg)	0.0		H5C2═H8C3	1.0882	1.096
μ (Debyes)	4.5208		H6C2═H9C3	1.0901	1.097
μ_b (Debyes)	0.5062		H7C2═H10C3	1.0900	1.093
μ_c (Debyes)	4.4923		C3S1C2	95.7	96.56
A_e (MHz)	7031.4237		O4S1C2═O4S1C3	106.5	106.6
B_e (MHz)	6983.4721		H5C2S1═H8C3S1	107.0	109.49
C_e (MHz)	4252.9289		H6C2S1═H9C3S1	108.5	110.06
(A_e + B_e)/2	7007.4479		H7C2S1═H10C3S1	109.9	110.84
κ (equil)	0.965484		α	64.9	64.49
A_0 (MHz)	7031.7237	7036.5822165(234)	H5C2S1C3	176.9	178.01
B_0 (MHz)	6920.1221	6910.8301279(228)	H8C3S1C2	183.11	181.99
C_0 (MHz)	4223.3389	4218.776511(44)	H6C2S1H5═H10C3S1H8	119.5	119.2
(A_0 + B_0)/2	6975.9229	6973.7062	H7C2S1H5═H9C3S1H8	−118.6	−120.1
κ(ZPVE)	0.920523				

[a]The experimental values of ref 16 have been determined from using the experimental rotational constants of eight isotopomers measured at the ground vibrational states.

DOI: 10.1021/acs.jpca.5b06941
J. Phys. Chem. A 2015, 119, 9644−9652

Table 2. Equilibrium Rotational Constants, B_e, and ΔB_e^{CORE} and ΔB_{vib} (MHz)

set	method	N	$A_e(x)$	$B_e(y)$	$C_e(z)$
I	CCSD(T)-F12/VTZ-F12	8	7031.4237	6983.4721	4252.9289
II	CCSD(T)/cc-pCVTZ	8	6961.1142	6940.5093	4220.5948
III	CCSD(T)/cc-pCVTZ	1	6985.5018	6961.9183	4234.3415
IV	CCSD(T)/cc-pCVTZ	0	6986.8960	6962.5960	4234.9894
		ΔA_e^{CORE}	ΔB_e^{CORE}		ΔC_e^{CORE}
B_e(III) − B_e(II)		24.39	21.41		13.75
B_e(IV) − B_e(II)		25.78	22.09		14.39
		MP2/AVTZ			
B_{xe}	6929.854	$A_0(x)$	6901.367	$\Delta A_{vib} = A_0 - A_e$	−25.48
B_{ye}	6948.143	$B_0(y)$	6862.693	$\Delta B_{vib} = B_0 - B_e$	−85.44
B_{ze}	4219.561	$C_0(z)$	4175.572	$\Delta C_{vib} = C_0 - C_e$	−43.98

[a] N = inner orbitals excluded from the correlation calculation.

Table 3. CCSD(T)-F12b Harmonic Frequencies (ω, cm^{-1}), MP2 Anharmonic Fundamentals (ν, cm^{-1}), Estimated Band Centers (ν, cm^{-1}), and IR (Harmonic) Intensities [I, D^2/(Å^2 amu)]

	mode		CCSD(T)-F12 VTZ-F12 ω	MP2 AVTZ ν	estimated band centers (CC/MP2) ν	I (MP2)	exp[ref] (gas phase)
A′	ν_1	*CH$_3$ s*	3156	3054	3017	1.14	3001;[14] 3010[15]
	ν_2	*CH$_3$ s*	3147	3045	3007	4.28	3001;[14] 3010[15]
	ν_3	*CH$_3$ s*	3042	2958	2932	6.14	2922;[14] 2933[15]
	ν_4	*CH$_3$ b*	1485	1451	1440	17.35	1440;[14] 1455[15]
	ν_5	*CH$_3$ b*	1463	1427	1418	4.39	1419;[14] 1440[15]
	ν_6	*CH$_3$ b*	1343	1306	1306	10.92	1310;[14] 1319[15]
	ν_7	S−O s	1147	1101	1136	149.03	1101;[14] 1102[15]
	ν_8	HCS b	1032	1011	1007	13.59	1004;[14] 1016[15]
	ν_9	*CH$_3$ b*	964	946	943	6.50	930;[14] 953[15]
	ν_{10}	CS s	677	666	659	7.96	661;[14] 672[15]
	ν_{11}	SO w	377	369	**377**	6.88	**376.751**;[5] 376;[14] 382;[c,15] 388.7;[c,17] 363[c,19]
	ν_{12}	CSC b	291	289	291	0.36	308;[c,15] 306.5;[c,17] 303;[c,19] 308[d,5]
	ν_{13}	*CH$_3$ t*	244	232	229	0.33	212;[c,15] 219.5;[c,17] 231;[c,19] 231[d,5]
A″	ν_{14}	*CH$_3$ s*	3156	3054	3016	0.31	3001;[14] 3010[15]
	ν_{15}	*CH$_3$ s*	3144	3042	3004	0.01	3001;[14] 3010[15]
	ν_{16}	*CH$_3$ s*	3041	2960	2933	2.20	2922;[14] 2933[15]
	ν_{17}	*CH$_3$ b*	1465	1431	1420	0.03	1419[15]
	ν_{18}	*CH$_3$ b*	1448	1414	1405	8.97	1404;[14] 1405[15]
	ν_{19}	*CH$_3$ b*	1322	1287	1286	1.86	1293;[14] 1304[15]
	ν_{20}	*CH$_3$ b*	932	920	912	6.50	915;[14] 933[15]
	ν_{21}	HCS b	893	887	876	2.23	881[14]
	ν_{22}	C−S s	701	689	683	14.38	685;[14] 695[15]
	ν_{23}	OSC b	322	316	**322**	8.31	**323.988**;[5] 333;[c,14,15] 331.3;[c,17] 347[c,19]
	ν_{24}	*CH$_3$ t*	186	187	183	0.0	212;[c,15] 201.9;[c,17] 207;[c,19] 207[d,5]

[a] s = stretching; b = bending; *t* = torsion, w = wagging = in-plane bending; *italic* = important Fermi displacements. [b] $\Delta\nu$ = Fermi displacements (emphasized in bold if $\Delta\nu$ > 10 cm^{-1}). [c] Predicted form semiempirical force fields. [d] Anharmonic fundamentals calculated using DFT or ab initio methods.

MP2/AVTZ level of theory using the algorithms implemented in the code Gaussian 09.[28] Then, anharmonic properties are predicted with VPT2.[29] Because anharmonic effects are less dependent on the level of electronic structure theory than the zero-order properties (i.e., equilibrium rotational constants and harmonic frequencies), we combined two different levels of theory to determine the band centers of all the vibrational fundamentals and to calculate rotational constants in the excited vibrational levels. CCSD(T)-F12b was employed for the zero-order properties and MP2 theory is used for anharmonicities. Resulting frequencies and intensities are shown in Tables 3 and 4. Intensities are determined within the harmonic approximation.

The predicted band positions are in very good agreement with previous experimental data. For the lower frequency modes ν_{11} (SO in-plane) and ν_{23} (OSC out-of-plane bending), our calculations predict the fundamental frequencies to be 377 and 322 cm^{-1}, very close to the very recent values of Cuisset et al.[5] (376.751 and 323.988 cm^{-1}). The agreement between theory and calculations confirms (definitively) these band center positions.

Bands for the remaining large amplitude modes, whose intensities are expected to be very low, have not been observed. Previous data are more or less accurate estimations. The ν_{12} fundamental transition (CSC bending) was predicted to lie at 291 cm^{-1}, below previous assessments (303−308 cm^{-1} [5,15,17,19]). On the contrary, the two torsional modes ν_{13}

DOI: 10.1021/acs.jpca.5b06941
J. Phys. Chem. A 2015, 119, 9644−9652

Table 4. Rotational Constants Calculated in the Excited Vibrational States and Centrifugal Distortion Constants Computed with MP2/AVTZ

Ground and Excited Vibrational State Rotational Constants (MHz)										
	mode[a]		estimated band centers (cm^{-1})		ΔB_x		ΔB_y		ΔB_z	
sym			VPT2	variat[b]	calc	ref 4	calc	ref 4	calc	ref 4
A′	ν_{11}	SO w	377		3.42	5.01	8.87	3.59	−0.24	−1.04
	ν_{12}	CSC b	291		26.14	23.98	−12.62	−13.59	−29.95	−27.39
	ν_{13}	*CH3 t*	229	229.8	1.89	1.22	−35.68	−31.78	−8.48	−8.25
A″	ν_{23}	OSC b	322		−1.05	0.87	−0.57	−6.87	16.46	11.97
	ν_{24}	*CH3 t*	183	192.3	−6.90	−6.68	−9.89	−11.57	−4.95	−5.35

Ground Vibrational State Centrifugal Distortion Constants S-Reduction Hamiltonian					
		calc	exp[4]	exp[7]	
		I^r	III^r	I^r	III^r
Δ_J (kHz)		3.030030	6.0889172(164)	3.463079(14)	6.089201(16)
Δ_K (kHz)		4.133114	3.989536(48)	3.767553(89)	3.989320(37)
Δ_{JK} (kHz)		−0.00639	−8.938057(49)	−0.925893(71)	−8.937244(53)
d_1 (kHz)		−1.223187	−0.1639913(103)	−1.4548584(69)	0.164061(11)
d_2 (kHz)		−0.279661	−0.2717076(58)	−0.2939137(42)	−0.2717127(48)
H_J (Hz)		−0.002288	0.0088016(81)	−0.0027288(53)	0.0088720(43)
H_K (Hz)		0.220185	−0.0219640(256)	0.085683(80)	−0.0021331(15)
H_{JK} (Hz)		0.084525	−0.0396809(242)	0.051058(41)	−0.038929(21)
H_{KJ} (Hz)		−0.299169	0.052778(37)	−0.116535(87)	0.0051699(27)
h_1 (Hz)		0.001571	−0.0017637(63)	0.0012583(22)	0.016709(38)
h_2 (Hz)		0.000972	0.00110658(51)	0.0026560(23)	0.0010231(23)
h_3 (Hz)		−0.001914	−0.00137384(224)	−0.00011300(68)	0.00134332(85)

Ground Vibrational State Centrifugal Distortion Constants A-Reduction Hamiltonian			
	calc	exp[7]	
	I^r	I^r	III^r
Δ_J (kHz)	3.589623	4.050907(14)	6.62679(10)
Δ_K (kHz)	6.922722	6.706545(70)	6.67255(37)
Δ_{JK} (kHz)	−3.362324	−4.452825(45)	−12.15739(44)
δ_J (kHz)	1.223187	1.4548677(66)	−0.164790(83)
δ_K (kHz)	1.136236	1.285585(18)	−46.8755(53)
Φ_J (Hz)	−0.000345	0.0025809(39)	0.006694(29)
Φ_K (Hz)	0.147610	0.080893(66)	−2.71655(68)
Φ_{JK} (Hz)	0.042664	0.017314(23)	−1.17573(35)
Φ_{KJ} (Hz)	−0.185776	−0.083466(57)	3.8841(10)
ϕ_J (Hz)	−0.000343	0.0011453(19)	0.002600(30)
ϕ_K (Hz)	−0.030560	0.004977(16)	−0.9056(31)
ϕ_{JK} (Hz)	0.020103	0.0082096	−0.16266(46)

[a] *italic* = important Fermi displacements. [b] The "variational" band centers have been estimated using CCSD(T)-F12 theory.

and ν_{24} were calculated to be 229 and 183 cm^{-1}, respectively. Whereas ν_{13} is in good agreement with previous data (231 cm^{-1} [5,19]), the low-intensity band ν_{24} fundamental is determined to be very far away from previous estimations (all of them above 200 cm^{-1} [5,15,17,19]). For more comments, variational procedures as the one that we describe in next sections are needed. VPT2 represents only a first approximation unable for the treatment of splittings and barrier effects for internal rotation modes.

In Table 4, the relative values of the rotational constants for five low-frequency fundamentals referred to those of the ground vibrational state are shown and compared with the experimental results of Cuisset et al.[4] They are not ordered following a rational criterion. We follow the order of the equilibrium rotational constants, which varies with the vibrational excitations. In addition, Table 4 shows ab initio centrifugal distortion constants calculated using the (S, I^r)-reduction. The previous experimental data of Cuisset et al.[4] and Margulès et al.[7] are also shown. These last are used for comparison, because ref 7 provides various sets of parameters: (S, I^r), (A, I^r), (S, III^r), and (A, III^r). Our ab initio ones calculated with the (A, I^r) model are in better agreement with the data of ref 7 than those corresponding to the symmetrically reduced model.

Torsional Modes and the Far Infrared Spectrum. Torsional energy levels were determined variationally assuming very small, almost negligible, interactions between the two large amplitude torsional modes and the remaining vibrations. The VPT2 full-dimensional analysis supports this approximation because Fermi displacements of the low torsional energies and the levels of the remaining vibrational modes are not expected.

Thus, the following 2-dimensional Hamiltonian can be defined to be solved variationally:[23−26]

DOI: 10.1021/acs.jpca.5b06941
J. Phys. Chem. A 2015, 119, 9644−9652

Table 5. Torsional Potential[a] and Kinetic Parameters of DMSO (cm^{-1})

	CCSD(T)/AVTZ	CCSD(T)-F12/VTZ		
	E	E	E^{eff}	exp[19]
$V_3 = [E(60,0) - E(0,0)]$	980.64	956.41	965.32	951.1
$[E(60,60) - E(0,0)]$	2266.97	2184.99	2212.16	
$[E(60,60) - E(60,0) - E(0,60)]$	305.69	272.17	281.52	
C^{cc}	70.338	68.084	70.379	
C^{ss}	−95.475	−95.447	−100.489	
B_{11}	5.4839	5.4749		
B_{22}	5.4839	5.4749		
B_{12}	−0.0347	−0.0383		

[a] C^{cc} and C^{ss} are the expansion coefficients of the $\cos 3\theta_1 \cos 3\theta_2$ and $\sin 3\theta_1 \sin 3\theta_2$ terms 2D-PES.

$$\hat{H}(\theta_1,\theta_2) = -\sum_{i=1}^{2}\sum_{j=1}^{2}\left(\frac{\partial}{\partial\theta_i}\right)B_{\theta_i\theta_j}(\theta_i,\theta_j)\left(\frac{\partial}{\partial\theta_j}\right) + V^{eff}(\theta_1,\theta_2) \quad (2)$$

Here, the independent coordinates θ_1 and θ_2 are identified as the two CH_3 torsions (Figure 1). The definition of the torsional coordinates to use them for a partial optimization of the geometry is not obvious.[40] These vibrational coordinates were defined as a function of some dihedral angles using the following equations (for the labeling of the atoms, see Figure 1):

$$\theta_1 = (\text{H5C2S1C3} + \text{H6C2S1C3} + \text{H7C2S1C3})/3 - \pi$$
$$\theta_2 = (\text{H8C3S1C2} + \text{H9C23S1C2} + \text{H10C2S1C2})/3 - \pi \quad (3)$$

In eq 2, $B_{\theta1\theta2}(\theta_1,\theta_2)$ and $V^{eff}(\theta_1,\theta_2)$ represent the kinetic energy parameters and the effective potential energy surface, respectively. This last can be defined as

$$V^{eff}(\theta_1,\theta_2) = V(\theta_1,\theta_2) + V'(\theta_1,\theta_2) + V^{ZPVE}(\theta_1,\theta_2) \quad (4)$$

where $V(\theta_1,\theta_2)$ is the 2D-PES surface, $V'(\theta_1,\theta_2)$ the pseudopotential, and $V^{ZPVE}(\theta_1,\theta_2)$ represents the zero point vibrational energy correction. For more details about the definitions of V' and V^{ZPVE} and their computation, see refs 23−26.

In this paper, the 2D-PES was determined from the CCSD(T)-F12/VTZ-F12 total electronic energies of 16 conformations chosen for different values of θ_1 and θ_2 (θ_1, θ_2 = 0°, +90°, −90°, +180°). In all the selected geometries, $3N^a - 6 - 2$ internal coordinates (N^a = number of atoms) were optimized at the CCSD(T)-F12 level of theory. All the optimized conformations were inputs for the computation of the pseudopotential and the kinetic energy parameters.[23]

The determination of the V^{ZPVE} is computationally expensive because it implies to determine vibrational frequencies using all the 16 optimized geometries. However, it has a low dependence on the correlation energy. For this reason, it was computed at the MP2/AVTZ level of theory within the harmonic approximation.

The parameters, calculated for all the geometries, were fitted to totally symmetric double Fourier series. Thus, the effective PES is

$$\begin{aligned} V^{eff}(\theta_1,\theta_2) = {} & 1059.563 - 558.655(\cos 3\theta_1 + \cos 3\theta_2) \\ & + 70.379 \cos 3\theta_1 \cos 3\theta_2 - 11.408(\cos 6\theta_1 + \cos 6\theta_2) \\ & + 5.616(\cos 6\theta_1 \cos 3\theta_2 + \cos 3\theta_1 \cos 3\theta_2) \\ & - 2.027 \cos 6\theta_1 \cos 6\theta_2 - 100.489 \sin 3\theta_1 \sin 3\theta_2 \\ & + 4.293(\sin 3\theta_1 - \sin 3\theta_2) \\ & - 4.924(\cos 3\theta_1 \sin 3\theta_2 - \sin 3\theta_1 \cos 3\theta_2) \\ & - 1.850(\cos 6\theta_1 \sin 3\theta_2 - \sin 3\theta_1 \cos 6\theta_2) \end{aligned} \quad (5)$$

In Table 5, the most relevant potential energy parameters, as well as B_{11}, B_{22}, and B_{12}, the independent coefficients of the kinetic energy parameters, $B_{\theta1\theta2}(\theta_1,\theta_2)$, are shown. The methyl torsional barrier V_3 (Figure 2A,B) has been calculated to be

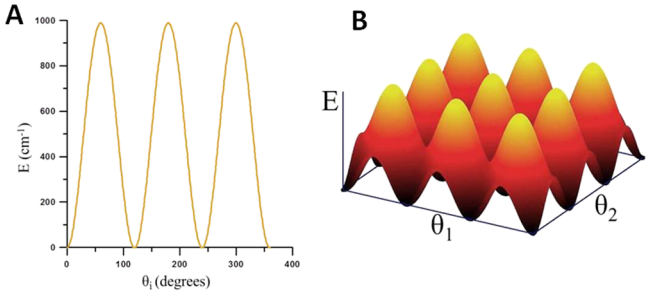

Figure 2. (A) One-dimensional cut of the torsional potential energy surfaces. (B) Two-dimensional energy surface depending on the two torsional angles θ_1 and θ_2.

956.41 and 965.32 cm^{-1} from the $V(\theta_1,\theta_2)$ and $V^{eff}(\theta_1,\theta_2)$ surfaces in very good agreement with the semiempirical value (2.94 kcal/mol = 951.1 cm^{-1}) of Dreizler and Dendl.[19] In the same table, we emphasize the $[E(60,60) - E(60,0) - E(0,60)]$ parameter and the expansion coefficients of the $\cos 3\theta_1 \cos 3\theta_2$ and $\sin 3\theta_1 \sin 3\theta_2$ terms of the 2D-PES. The three properties reflect the interactions between both torsional modes. C^{ss} and B_{12} (−100.489 cm^{-1}; −0.0383 cm^{-1}) are the origin of the $\nu_{13}-\nu_{24}$ gap calculated to be 37.5 cm^{-1}.

In DMSO, the kinetic contribution to the interaction between both CH_3 molecules is very small, in spite of the potential contribution that is really large in comparison with other sulfur organic molecules such as DMS (C^{ss} = 6.1; B_{12} = −0.30).[41] The $[E(60,60) - E(60,0) - E(0,60)]$ difference, which denotes the relevance of this interaction, is small in DMS (2.4 cm^{-1}) and really large in DMSO (281.5 cm^{-1}). In both species, the long CS distances (CS = 1.8 Å) force the separation of the two rotating groups to avoid interactions. However, in

DOI: 10.1021/acs.jpca.5b06941
J. Phys. Chem. A 2015, 119, 9644−9652

Table 6. Low Torsional Energy Levels (cm^{-1}) of DMSO Calculated at the CCSD(T)-F12/VTZ-F12 Level of Theory

ν_{24} ν_{13}	sym	calc	exp[b]	ν_{24} ν_{13}	sym	calc	ν_{24} ν_{13}	sym	calc
0 0	A_1	0.000[a]	0.0	0 2	A_1	452.037	4 0	A_1	724.101
	G	0.001			G	452.056		G	724.228
	E_1	0.000			E_1	452.071		E_1	730.821
	E_3	0.000			E_3	452.071		E_3	730.814
1 0	A_2	192.317	202−212	3 0	A_2	566.458	3 1	A_2	724.361
	G	192.317			G	566.191		G	731.050
	E_2	192.315			E_2	565.950		E_2	731.278
	E_3	192.315			E_3	565.950		E_3	731.285
0 1	A_1	229.837	231	2 1	A_1	573.641	2 2	A_1	778.027
	G	229.837			G	573.265		G	778.528
	E_1	229.835			E_1	572.865		E_1	779.038
	E_3	229.835			E_3	572.864		E_3	779.037
2 0	A_1	382.573		1 2	A_2	611.834	1 3	A_2	806.982
	G	382.589			G	611.604		G	807.469
	E_1	382.603			E_2	611.368		E_2	807.935
	E_3	382.603			E_3	611.368		E_3	807.937
1 1	A_2	403.808		0 3	A_1	665.716	0 4	A_1	868.613
	G	403.839			G	665.609		G	846.285
	E_2	403.868			E_1	665.495		E_1	846.698
	E_3	408.868			E_3	665.495		E_3	845.821

[a]ZPVE = 217.552 cm^{-1}, [b]See last column of Table 3.

DMSO, the CSC angle (95.7°) is smaller than in DMS (98.6°)[41] approaching the hydrogen atoms of the two methyl groups.

In Table 6, the torsional energy levels calculated variationally are shown. The levels are classified using the representation of the G_{18} group. Each level splits into nine components which are nondegenerate, degenerate, or pseudodegenerate.

The G components of the torsional levels are expected to show the high intensities given the nuclear spin statistical weights. The fundamentals have been calculated to be 229.837 cm^{-1} (ν_{13}) and 192.317 cm^{-1} (ν_{24}). Whereas ν_{13} is in good agreement with previous estimations (~231 cm^{-1} [4,19]), the calculated value for ν_{24}, in spite of it being higher than the VTP2 one (183 cm^{-1}), is too low in comparison with previous assessments that place the band above 200 cm^{-1}.[5,15,17,19] Because there are not direct observations of this band whose intensity is predicted to be very low, we propose a new assignment on the basis of ab initio calculations. According to this new assignment that takes into consideration the deviation of present theoretical procedures and our experience in the study of torsional frequencies, the ν_{24} fundamental can be predicted to lie between 190 and 195 cm^{-1}.

Finally, Table 7 collects predictions for the band center positions lying below 650 cm^{-1}. We followed three different procedures to determine them. The torsional transitions $N\nu_{23}$, $N'\nu_{24}$, and $N\nu_{23} + N'\nu_{24}$ were calculated from the variational torsional energy levels of Table 6. Overtones and combination bands involving the ν_{11}, ν_{12}, and ν_{23}, modes are derived from VPT2.[29] Combination transitions involving one bending mode and one torsional mode were calculated using the VPT2 and variational fundamentals of Tables 3 and 6, and the equation $\nu_N + \nu_N$. The torsional modes and the bending modes are assumed on the basis of the VPT2 results.

Because, except for ν_{11} and ν_{23}, experimental information for these band center frequencies is poor or missing, our predictions, being the most accurate to date, may help to resolve the outstanding problem of the rotational spectroscopy of DMSO, notably the nature of the "dark state"[5] perturbing ν_{11}

Table 7. Estimated Band Centers Lying in the Far Infrared Region below 650 cm^{-1}

	variational[a]	VPT2[b]	$\nu_N + \nu_{N'}$[c]	exp[5]
ν_{24}	192.3			
ν_{13}	229.8			
ν_{12}		291		
ν_{23}		322		323.988
ν_{11}		377		376.751
$2\nu_{24}$	382.6			
$\nu_{13} + \nu_{24}$	403.8			
$2\nu_{13}$	452.1			
$\nu_{24} + \nu_{12}$			483	
$\nu_{24} + \nu_{23}$			514	
$\nu_{13} + \nu_{12}$			521	
$\nu_{13} + \nu_{23}$			552	
$3\nu_{24}$	556.2			
$\nu_{24} + \nu_{11}$			569	
$\nu_{13} + 2\nu_{24}$	573.3			
$2\nu_{12}$		583		
$\nu_{13} + \nu_{11}$			607	
$2\nu_{13} + \nu_{24}$	611.6			
$\nu_{12} + \nu_{23}$		613		
$2\nu_{23}$		644		
$3\nu_{13}$	665.6			
$\nu_{11} + \nu_{12}$		668		

[a]Calculated from the energies of Table 6. [b]Estimated using VPT2, a CCSD(T)-F12 harmonic force field, and an MP2 anharmonic force field. [c]Estimated from the VPT2 frequencies of Table 3 and the variational levels of Table 6.

at J = 30−40. According to our calculations, the $2\nu_{24}$ overtone predicted to lie 6 cm^{-1} above ν_{11} is the best candidate. In Figure 3, we attempted to superimpose the rotational structures of $2\nu_{24}$ and ν_{11}.

The neighbor state ν_{23} is also indicated. The scalar term, $0.5(E_{A(J)} + E_{C(J)}) \sim BJ(J+1) + ...$, is deduced from all energies. We can confirm that for J = 30−40, both states tend to align closely

DOI: 10.1021/acs.jpca.5b06941
J. Phys. Chem. A 2015, 119, 9644−9652

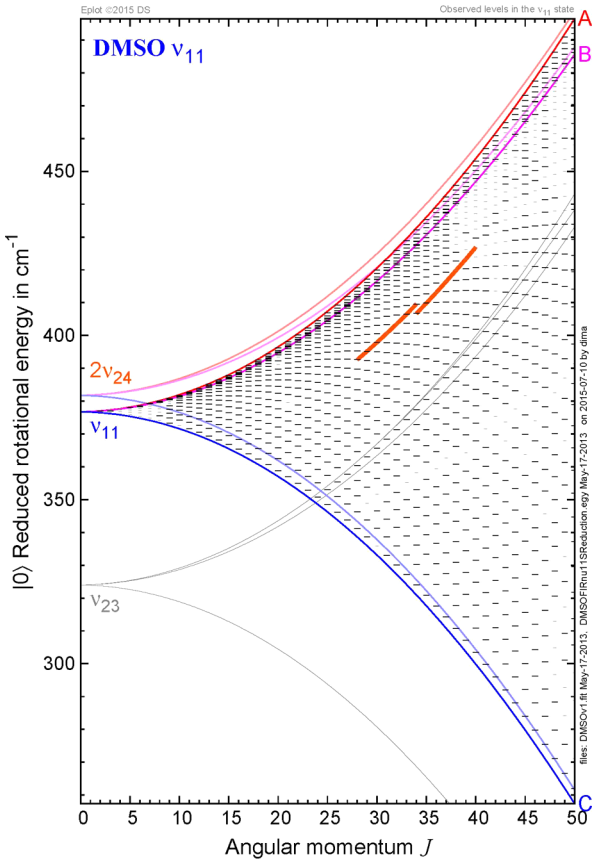

Figure 3. Rotational structure of the ν_{11} fundamental state of DMSO (observed at 376.751 cm^{-1}) and the envelope of the possible rotational multiplet of the potential perturbed state $2\nu_{24}$, the "dark state" (calculated at 382.6 cm^{-1}). Red, purple, and blue solid lines give energies of classical stationary rotation about principal axes *A*, *B*, and *C*, respectively. Dashes represent quantum states; longer dashes mark states observed in refs 3 and 5. Two bold solid orange lines mark the region where strong perturbations by the "dark state" have been observed.[5]

and crossings of sequences of quantum states should occur. Furthermore, a low-order interaction (in particular, Fermi resonances) may become sufficiently strong to be uncovered explicitly.

CONCLUSIONS

The aim of this paper is to obtain as much information as possible derived from highly correlated ab initio methods (CCSD(T)-F12) that can be relevant for further assignments of the DMSO rotational spectra. Two features can be emphasized:

(1) The singular structure and dynamic properties of DMSO lead to intricate assignments of the rotational spectra. DMSO is a near the oblate top where equilibrium rotational constants obey the $A_e \sim B_e > C_e$ relation. Ab initio calculations allow us to assert that DMSO rotational constants are strongly dependent on anharmonic effects. Asymmetry increases with the vibrational energy. For the ground vibrational state, these parameters were calculated to be A_0 = 7031.7237 MHz, B_0 = 6920.1221 MHz, and C_0 = 4223.3389 MHz, a few megahertz from the previous experimental measurements.

(2) Previous assignments of the two torsional fundamentals of DMSO are uncertain. In this paper, torsional energies and transitions were computed variationally. Whereas the ν_{13} torsional fundamental was found to lie at 229.837 cm^{-1} in good agreement with previous assessment, there is no agreement for ν_{24}. For this low intense transition, a new assignment that predicts the band center to lie between 190 and 195 cm^{-1}, is proposed.

Finally, the vibrationally corrected V_3 torsional barrier was evaluated to be 965.32 cm^{-1} and the torsional splitting of the ground vibrational state has been estimated to be lower than 0.01 cm^{-1}.

AUTHOR INFORMATION

Corresponding Author

*M. L. Senent. E-mail: senent@iem.cfmac.csic.es.

Present Address

†S. Dalbouha. LS3ME-Equipe de Chimie Théorique et Modélisation, Université Mohamed V - Agdal, Faculté des Sciences Rabat, Morocco. E-mail: samiradalbouha@gmail.com

Notes

The authors declare no competing financial interest.

‡A. Cuisset. E-mail: arnaud.cuisset@univ-littoral.fr

§D. Sadovskii. E-mail: sadovski@univ-littoral.fr

ACKNOWLEDGMENTS

This research was supported by the MINECO of Spain grant FIS2013-40626-P and by a Marie Curie International Research Staff Exchange Scheme Fellowship within the seventh European Community Framework Program under grant no. PIRSES-GA-2012-31754. The authors acknowledge the COST Actions CM1405 "MOLIM" and CM1401 "Our Astrochemical History". The authors are also involved in the International Group (GDRI) HIGHRESMIR. The authors acknowledge the CTI (CSIC) and CESGA for computing facilities.

REFERENCES

(1) Arsene, C.; Barnes, I.; Becker, K. H.; Schneider, W. F.; Wallington, T. T.; Mihalopoulos, N.; Patroescu-Klotz, I. V. Formation of Methane Sulfinic Acid in the Gas-Phase OH-Radical Initiated Oxidation of Dimethyl Sulfoxide. *Environ. Sci. Technol.* **2002**, *36* (23), 5155−5163.

(2) Sørensen, S.; Falbe-Hanse, H.; Mangoni, M.; Hjorth, J.; Jensen, N. Observation of DMSO and $CH_3S(O)OH$ from the Gas Phase Reaction Between DMS and OH. *J. Atmos. Chem.* **1996**, *24*, 299−315.

(3) Cuisset, A.; Nanobashvili, L.; Smirnova, I.; Bocquet, R.; Hindle, F.; Mouret, G.; Pirali, O.; Roy, P.; Sadovskiĭ, A. D. Far- infrared High Resolution Synchrotron FTIR Spectroscopy of the ν_{11} Bending Vibrational Fundamental Transition of Mimethylsulfoxyde. *Chem. Phys. Lett.* **2010**, *492*, 30−34.

(4) Cuisset, A.; Martin Drumel, M.-A.; Hindle, F.; Mouret, G.; Sadovskiĭ, D. A. Rotational Structure of the Five Lowest Frequency Fundamental Vibrational States of Dimethyl Sulfoxide. *Chem. Phys. Lett.* **2013**, *586*, 10−15.

(5) Cuisset, A.; Sadovskiĭ, D. A. Gyroscopic Destabilization in Polyatomic Molecules: Rotational Structure of the Low Frequency Bending Vibrational States ν_{23} and ν_{11} of Dimethyl Sulfoxide. *J. Chem. Phys.* **2013**, *138*, 234302.

(6) Cuisset, A.; Pirali, O.; Sadovskiĭ, D. A. Gyroscopic Destabilization of Molecular Rotation and Quantum Bifurcation Observed in the Structure of the ν_{23} Fundamental of Dimethyl Sulfoxyde. *Phys. Rev. Lett.* **2012**, *109*, 094101.

DOI: 10.1021/acs.jpca.5b06941
J. Phys. Chem. A 2015, 119, 9644−9652

(7) Margulès, L.; Motiyenko, R. A.; Alekseev, E. A.; Demaison, J. Choice of the Reduction and of the Representation in Centrifugal Distortion Analysis: A Case Study of Dimethyl Sulfoxide. *J. Mol. Spectrosc.* **2010**, *260*, 23−29.
(8) Vogt, N.; Demaison, J.; Rudolph, H. D. Semiexperimental Equilibrium Structure of the Oblate-Top Molecules Dimethyl Sulfoxide and Cyclobutene. *J. Mol. Spectrosc.* **2014**, *297*, 11−15.
(9) Senent, M. L.; Smeyers, Y. G. Ab initio Calculations and Analysis of the Torsional Spectra of Dimethylamine and Dimethylphosphine. *J. Chem. Phys.* **1996**, *105*, 2789−2797.
(10) Aliev, M. R.; Watson, J. K. G. In *Molecular Spectroscopy: Modern Research*; Rao, K. N., Eds.; Academic Press: New York, 1985; Vol. *III*, p 1.
(11) Horrocks, W. D., J.r; Cotton, F. A. Infrared and Raman Spectra and Normal Co-ordinate Analysis of Dimethyl Sulfoxide and Dimethyl Sulfoxide-d_6. *Spectrochim. Acta, Part A* **1961**, *17*, 134−147.
(12) Salonen, A. K. *Raman and Infrared Spectra of Dimethyl Sulfoxide: Vibrations and Rotations*; Annales Academiae Scientiarum Fennicae; Suomalainen tiedeakatemia: Helsinki, 1961; Vol. *67*.
(13) Forel, M.-T.; Tranquille, M. Spectres de Vibration du Diméthyl Sulfoxyde et du Diméthyl Sulfoxyde-d_6. *Spectrochim. Acta* **1970**, *26A*, 1023−1034.
(14) Tranquille, M.; Labarbe, P.; Fouassier, M.; Forel, T. Determination des Champs de Force et des Modes Normaux de Vibration des Molecules $(CH_3)_2S$ et $(CH_3)_2SO$. *J. Mol. Struct.* **1971**, *8*, 273−291.
(15) Geiseler, G.; Hanschmann, G. Schwingungsverhalten von Dimethylsulfid, Dimethylsulfoxid, Dimithylsulfon und den Entsprechenden per Deuterierten Verbindungen. *J. Mol. Struct.* **1972**, *11*, 283−296.
(16) Typke, V. The r_s Structure of DMSO, Revisited. *J. Mol. Struct.* **1996**, *384*, 35−40.
(17) Typke, V.; Dakkouri, M. The Force Field and Molecular Structure of Dimethyl Sulfoxide from Spectroscopic and Gas Diffraction Data and Ab Initio Calculations. *J. Mol. Struct.* **2001**, *599*, 177−193.
(18) Cuisset, A.; Smirnova, I.; Bocquet, R.; Hindle, F.; Mouret, G.; Yang, C.; Pirali, O.; Roy, P. Gas Phase THz Spectroscopy of Toxic Agent Simulant Compounds using the AILES Synchrotron Beamline. *AIP Conf. Proc.* **2009**, *1214*, 85−89.
(19) Dreizler, H.; Dendl, G. Bestimmung des Hinderungspotentials der internen Rotation aus dem Mikrowellenspektrum von Dimethylsulfoxyd. *Z. Naturforsch., A: Phys. Sci.* **1965**, *20* (11), 1431−1440.
(20) Knizia, G.; Adler, T. B.; Werner, H.-J. Simplified CCSD (T)-F12 Methods: Theory and Benchmarks. *J. Chem. Phys.* **2009**, *130*, 054104−1−20.
(21) Werner, H.-J.; Adler, T. B.; Manby, F. R. General Orbital Invariant MP2-F12 Theory. *J. Chem. Phys.* **2007**, *126*, 164102−1−18.
(22) Dalbouha, S.; Senent, M. L.; Komiha, N. Theoretical Spectroscopic Characterization at Low Temperatures of Methyl Hydroperoxide and various S-analogs. *J. Chem. Phys.* **2015**, *142*, 074304.
(23) Senent, M. L. Determination of the Kinetic Energy Parameters of Non-Rigid Molecules. *Chem. Phys. Lett.* **1998**, *296*, 299−306.
(24) Senent, M. L. Ab Initio Determination of the Roto-torsional Energy Levels of trans-1, 3-Butadiene. *J. Mol. Spectrosc.* **1998**, *191*, 265−275.
(25) Senent, M. L. Ab Initio Determination of the Torsional Spectra of Acetic Acid. *Mol. Phys.* **2001**, *99* (15), 1311−1321.
(26) Senent, M. L. Ab Initio Determination of the Torsional Spectrum of Glycolaldehyde. *J. Phys. Chem. A* **2004**, *108* (30), 6286−6293.
(27) Werner, H.-J.; Knowles, P. J.; Manby, F. R.; Schütz, M.; Celani, P.; Knizia, G.; Korona, T.; Lindh, R.; Mitrushenkov, A.; Rauhut, G.; et al. *MOLPRO*, version 2012.1 , a package of ab initio programs; see http://www.molpro.net.
(28) Frisch, M. J.; Trucks, G. W.; Schlegel, H. B.; Scuseria, G. E.; Robb, M. A.; Cheeseman, J. R.; Scalmani, G.; Barone, V.; Mennucci, B.; Petersson, G. A.; et al. *Gaussian 09*, Revision A.02; Gaussian, Inc.: Wallingford, CT, 2009.
(29) Barone, V. Anharmonic vibrational properties by a fully automated second-order perturbative approach. *J. Chem. Phys.* **2005**, *122*, 014108.
(30) Kendall, R. A.; Dunning, T. H., Jr; Harrison, R. J. Electron Affinities of the First Row Atoms Revisited. Systematic Basis Set and Wave Functions. *J. Chem. Phys.* **1992**, *96*, 6796.
(31) Peterson, K. A.; Adler, T. B.; Werner, H.-J. Systematically Convergent Basis Sets for Explicitly Correlated Wavefunctions: The atoms H, He, B−Ne, and Al−Ar. *J. Chem. Phys.* **2008**, *128*, 084102.
(32) Yousaf, K. E.; Peterson, K. A. Optimized Auxiliary Basis Sets for Explicitly Correlated Methods. *J. Chem. Phys.* **2008**, *129*, 184108−1−7.
(33) Raghavachari, K.; Trucks, G. W.; Pople, J. A.; Head-Gordon, M. A Fifth-Order Perturbation Comparison of Electron Correlation Theories. *Chem. Phys. Lett.* **1989**, *157*, 479−483.
(34) Woon, D. E.; Dunning, T. H., Jr. Gaussian Basis Sets for Use in Correlated Molecular Calculations. V. Core Valence Basis Sets for Boron Through Neon. *J. Chem. Phys.* **1995**, *103*, 4572−4585.
(35) Peterson, K. A.; Dunning, T. H., Jr. Accurate Correlation Consistent Basis Sets for Molecular Core−Valence Correlation Effects: The Second Row Atoms Al − Ar, and the First Row Atoms B−Ne Revisited. *J. Chem. Phys.* **2002**, *117*, 10548−10560.
(36) Senent, M. L. *ENEDIM, "A Variational Code for Non-Rigid Molecules"*; 2001 (see http://tct1.iem.csic.es/PROGRAMAS.htm for more details).
(37) Senent, M. L. The Symmetry of the Inversion-Bending Hamiltonian of Dimethyl-amine. *Int. J. Quantum Chem.* **1996**, *58* (4), 399−406.
(38) Senent, M. L.; Smeyers, Y. G.; Moule, D. C. An Ab Initio Three-Dimensional Torsion-Torsion-Bending Analysis of the Far Infrared Spectra of Dimethylamine. *J. Phys. Chem. A* **1998**, *102* (34), 6730−6736.
(39) Smeyers, Y. G.; Villa, M.; Senent, M. L. Ab Initio Determination of the Torsion-Wagging and Wagging-Bending Far Infrared Band Structure Spectra of Methylamine. *J. Mol. Spectrosc.* **1998**, *191*, 232−238.
(40) Inostroza, N.; Senent, M. L. Large amplitude vibrations of Urea in gas phase. *Chem. Phys. Lett.* **2012**, *524*, 25−31.
(41) Senent, M. L.; Puzzarini, C.; Domínguez-Gómez, R.; Carvajal, M.; Hochlaf, M. Theoretical Spectroscopic Characterization at Low Temperatures of Detectable Sulfur-Organic Compounds: Ethyl Mercaptan and Dimethyl Sulfide. *J. Chem. Phys.* **2014**, *140*, 124302.

DOI: 10.1021/acs.jpca.5b06941
J. Phys. Chem. A 2015, 119, 9644−9652